Effect of *B*-site randomness on the antiferroelectric/relaxor nature of the ground state: Diffuse and inelastic x-ray scattering study of $Pb(In_{1/2}Nb_{1/2})O_3$

Kenji Ohwada,[1,2,*] Shinya Tsukada,[3] Tatsuo Fukuda,[4] Satoshi Tsutsui,[5] Alfred Q. R. Baron,[6] Jun'ichiro Mizuki,[1,2] Hidehiro Ohwa,[7] Naohiko Yasuda,[7] and Hikaru Terauchi[2]

[1]*Synchrotron Radiation Research Center, Kansai Photon Science Institute, Quantum Beam Science Research Directorate, National Institutes for Quantum and Radiological Science and Technology, SPring-8, 1-1-1 Kouto, Sayo, Hyogo 679-5148, Japan*

[2]*School of Science and Technology, Kwansei Gakuin University, 2-1 Gakuen, Sanda, Hyogo 669-1337, Japan*

[3]*Faculty of Education, Shimane University, Matsue City, Shimane 690-8504, Japan*

[4]*Materials Sciences Research Center, Japan Atomic Energy Agency, SPring-8, 1-1-1 Kouto, Sayo, Hyogo 679-5148, Japan*

[5]*Japan Synchrotron Radiation Research Institute, SPring-8, 1-1-1 Kouto, Sayo, Hyogo 679-5198, Japan*

[6]*Materials Dynamics Laboratory, RIKEN SPring-8 Center, 1-1-1 Kouto, Sayo, Hyogo 679-5148, Japan*

[7]*Faculty of Engineering, Gifu University, 1-1 Yanagido, Gifu, Gifu 501-1193, Japan*

(Received 27 March 2018; revised manuscript received 18 June 2018; published 13 August 2018)

We have investigated the effect of *B*-site randomness on the antiferroelectric/relaxor nature of the ground state by studying diffuse and inelastic x-ray scattering from ordered and disordered $Pb(In_{1/2}Nb_{1/2})O_3$ (O- and D-PIN) single crystals. The diffuse scattering measurement of O-PIN, which is antiferroelectric at low temperatures, shows that the ferroelectrically interactive local polarization exists in the cubic phase, above the transition temperature T_N. Inelastic x-ray scattering analysis of the diffuse scattering shows that the transverse-acoustic (TA) and transverse-optic (TO) modes are dominant at high temperatures (∼800 K), while the central peak (CP) and TA modes, which are coupled, contribute majorly to diffuse scattering near T_N and show critical behavior at temperature close to T_N. The TO mode shows no anomaly at temperature close to T_N. Furthermore, the phonon spectra are broad, indicating that a strong damping mechanism exists even in the sample with weak chemical disordering, O-PIN. No clear difference between O- and D-PIN is observed at temperatures above ∼500 K. Here, the major difference between them is the property of the CP mode, which shows no drop and increases rapidly with decreasing temperatures in D-PIN. The CP mode is thought to be directly related to the local polarization and to originate in a combination of Pb flipping and the TO mode. The *B* site is considered to control the antiferroelectric/ferroelectric instability of lead-based perovskite materials. Finally, the *B*-site randomness is discussed in terms of suppressing the antiferroelectric instability and enhancing the polarization fluctuation.

DOI: 10.1103/PhysRevB.98.054106

I. INTRODUCTION

Relaxors, typified by $Pb(Mg_{1/3}Nb_{2/3})O_3$ (PMN) [1] and related materials, have attracted considerable scientific and industrial interest over the past few decades because they often show complex multiscale static and dynamic structures and puzzling mechanisms. They also show strong potential for industrial applications such as high-performance electromechanical transducers or capacitors based upon their good piezoelectric or dielectric properties.

From a structural viewpoint, it is generally accepted that the appearance of butterfly- or rod-shaped diffuse scattering around the Bragg position in reciprocal space is characteristic of and closely related to the relaxor states of lead-based perovskite oxides. Understanding the diffuse scattering and the related structures and dynamics of the polar (nano-) regions is one of the keys to understanding and defining the "relaxor" state. Despite long and intensive research, the origin and mechanism of the appearance of the diffuse scattering and the related dynamics remain under discussion [2,3].

The diffuse scattering and phonon instabilities result from complex interactions in the systems. Therefore, it is difficult to study them experimentally by measuring only the diffuse scattering and the phonon dynamics as they are. To overcome this difficulty, inelastic neutron and x-ray scattering measurements under field application [4–8] and continuous and fine tuning of the Ti composition in $Pb[(Mg_{1/3}Nb_{2/3})_{1-x}Ti_x]O_3$ (PMN-*x*PT) [9,10] have been proposed. Scattering measurements with randomness control [11,12], as will be shown in this paper, can also be an effective methodology for this purpose.

Chemical heterogeneities are seen at the perovskite *B* site in lead-based relaxor materials and are hereafter referred to as the *B*-site randomness. Lead-based relaxors have $PbB'B''O_3$ complex perovskite structures, where two different ions occupy the *B* site stoichiometrically to conserve the average charge of 4+ (charge neutrality in the system), for example, $Pb(Mg^{2+}_{1/3}Nb^{5+}_{2/3})O_3$ and $Pb(In^{3+}_{1/2}Nb^{5+}_{1/2})O_3$. However, the arrangement depends strongly on the materials. *B*-site randomness is commonly accepted to be intrinsic to the appearance of the relaxor state. The role of *B*-site randomness in relaxors has long been discussed. The effects of the random electric field in *heterovalent* PMN are discussed by means of a comparison with normal ferroelectrics such as

*ohwada.kenji@qst.go.jp

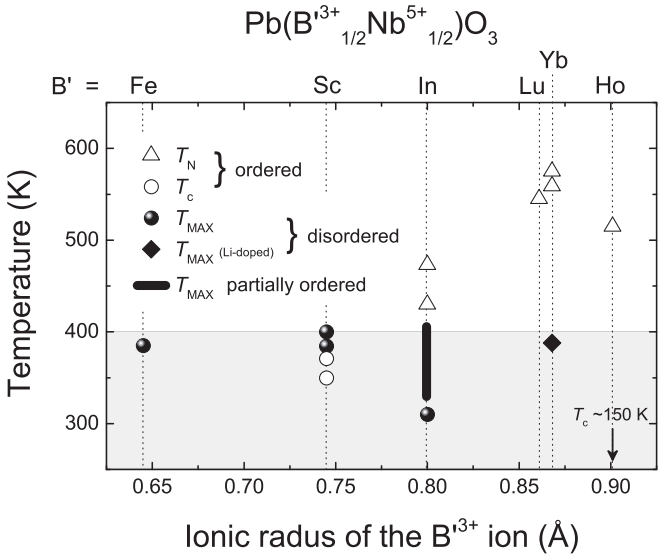

FIG. 1. Relationship between typical temperatures (T_N, T_C, T_{max}) and Shannon's ionic radius [16] of the B' ion in ordered and disordered $Pb(B'_{1/2}Nb_{1/2})O_3$. The ionic radii of Pb^{2+}, Nb^{5+}, and O^{2-}, which are common to all materials, are 1.49, 0.64, and 1.35 Å, respectively. The temperatures are representative; that is, they are not uniquely determined since they depend strongly on the sample preparation conditions and a slight change in B-site randomness results in a slight variation in temperature. The data are from Refs. [17–19] (for B' = Fe), [20–22] (for B' = Sc), [23–25] (for B' = In), [26] (for B' = Lu), [24,27,28] (for B' = Yb), and [29] (for B' = Ho).

homovalent $Pb(Zr^{4+}, Ti^{4+})O_3$ (PZT) [12]. The importance of these random electric fields has been explained by a few theories, such as random-field-induced domain states [13] and the spherical random-bond-random-field model [14]. However, random strain fields have been shown to be non-negligible. For instance, although it is not a lead-based material, $Ba(Zr^{4+}, Ti^{4+})O_3$ (BZT) is known to show the relaxor phenomena [15].

The $Pb(B'_{1/2}{}^{3+}Nb_{1/2}{}^{5+})O_3$ (B' = Fe, Sc, In, Lu, Yb, and Ho) series is interesting for investigating the effect of chemical heterogeneity on the antiferroelectric (AFE)/ferroelectric (FE)/relaxor nature of the ground state. All materials in this series contain Nb ions in common, and changing the B' ion results in a change in the strength of the random strain field owing to the different ionic radii of B' and Nb ions. Furthermore, the B-site randomness can be controlled by heat treatment if B' = Sc or In.

Figure 1 shows the relationship between typical temperatures (T_N, T_C, and T_{max}) and Shannon's ionic radius [16] of the B' ion in ordered and disordered $Pb(B'_{1/2}Nb_{1/2})O_3$. T_N and T_C denote the temperature of the AFE and FE phase transitions, respectively. T_{max} represents the temperature at which the dielectric constants are maximum. The ordered, disordered, and partially disordered terms will be used to show the degree of B-site randomness and will be described later. Notably, the phase-transition temperatures T_N and T_C tend to increase as the ionic radius of the B' ion increases. By contrast, between 300 and 400 K, T_{max} shows no clear dependence on ionic radius. This fact shows that the environment around the B site controls the phase-transition temperature and, presumably, the phase-transition type (AFE or FE). Furthermore, the polarization fluctuation resulting in T_{max} exists in the disordered case. Therefore, investigating the coupling between polarization fluctuation and B-site randomness is important for clarifying the appearance of the relaxor state, as well as that of the AFE and FE states.

$Pb(In_{1/2}Nb_{1/2})O_3$ (PIN) is a good material for this purpose. As mentioned previously, annealing of the PIN crystal results in ordering of the In and Nb atoms along the ⟨111⟩ direction, while quenching results in their disordering. Figure 2(a) shows the temperature-anneal-temperature (chemical order parameter S_2 [30,31]) phase diagram of $Pb(In_{1/2}Nb_{1/2})O_3$ [32]. PIN with a large In-Nb ordered region [$S_2 > 0.7$, ordered PIN (O-PIN)] transforms into an AFE state, while PIN with a large number of In-Nb disordered regions [$S_2 < 0.4$, disordered PIN (D-PIN)] becomes a relaxor [33]. It shows no clear phase transition at low temperature. The dielectric constant $\varepsilon'(T)$ exhibits a small but sharp drop at the transition temperature $T_N \sim 430$ K in the case of O-PIN [see Fig. 2(b)], while a large and broad peak around T_{max} near room temperature (RT) is seen in the case of D-PIN, where T_{max} depends strongly on the frequency of the external field [see Fig. 2(c)]. The partially ordered ($0.4 < S_2 < 0.7$) state is identified to show that the typical temperature (T_N or T_{max}) is widely distributed in the crystal [23,25], as shown in Fig. 1.

As shown in Figs. 2(b′) and 2(c′), from the viewpoint of x-ray scattering [11,30,34,35], the AFE state of O-PIN is characterized by $(\frac{h}{4}\frac{k}{4}0)$-type superlattice spots [Fig. 2(b′)], while the relaxor state of D-PIN is characterized by diffuse scattering along the ⟨101⟩ direction [Fig. 2(c′)], where the unit cell is the primitive-cubic cell ($a \sim 4.1$ Å) for comparison. However, the difference in the phonon dispersions between the two samples was not clear at RT [11]. The temperature evolution of the structures and related dynamics should be investigated to clarify the difference, that is, the effect of B-site randomness on the formation and growth processes of the polar regions.

In the present work, we focus on the temperature dependence of the phonon dynamics by measuring the diffuse and inelastic x-ray scattering (IXS) in O- and D-PIN single crystals. We start with O-PIN and focus on how the polarization appears and transforms into the AFE phase with temperature changes. Then, we move to D-PIN and try to find any differences induced by changing the B-site randomness.

II. EXPERIMENT

Single crystals of PIN were grown by the flux method from a mixture of PbO-In_2O_3-Nb_2O_5 [23]. The mixture was heated up to 1000 °C in a platinum crucible and held at this soak temperature for 5 h; then, the melt was cooled to 950 °C at a rate of 3 K/h, down to 800 °C at a rate of 5 K/h, and finally down to RT at a rate of 100 K/h. Typical sizes of the as-grown crystals were 1–2 mm, and the crystals were yellow in color. O-PIN was obtained by 20-h annealing at 650 °C, while D-PIN was obtained by quenching from 900 °C using liquid nitrogen.

The temperature dependence of the dielectric constants and $H0L$ mesh scans of O-PIN and D-PIN were measured, and the results were consistent with Figs. 2(b), 2(c) 2(b′), and 2(c′). Therefore, the O- and D-PIN samples prepared for the present

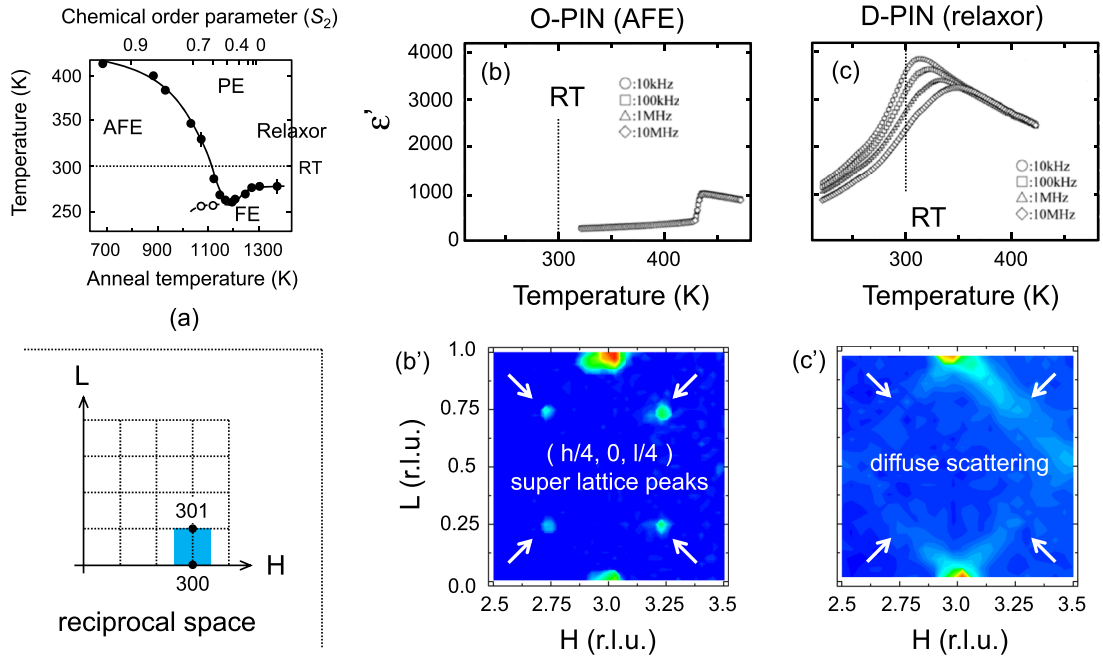

FIG. 2. (a) Temperature-anneal-temperature (chemical order parameter) phase diagram of $Pb(In_{1/2}Nb_{1/2})O_3$ [32]. Typical temperature dependence of the dielectric permittivity ϵ' of both (b) O- and (c) D-PIN [23]. $H0L$ mesh scans of (b′) O- and (c′) D-PIN are shown as well [11]. The inset shows that the reciprocal space corresponds to (b′) and (c′).

measurements were confirmed to be AFE and relaxor, respectively.

Detailed x-ray diffuse scattering measurement of O-PIN was performed at BL22XU in SPring-8 [36]. X-rays from an in-vacuum undulator were monochromatized using a liquid-nitrogen-cooled Si(111) double-crystal monochromator. The energy was tuned to 21.747 keV ($\lambda = 0.570$ Å), the same energy as that used for the dynamics measurement described below. A NaI scintillation counter was used as the detector.

The dynamics of O- and D-PINs were measured using the high-resolution IXS spectrometer at BL35XU in SPring-8 [37]. Data were collected using the Si (11 11 11) reflection at 21.747 keV, which provides an overall resolution of 1.6–1.8 meV depending on the analyzer crystal. The use of 12 analyzer crystals, 4 (horizontal) × 3 (vertical), placed at intervals of 120 mm at 9.8 m on the 2θ arm (horizontal scattering plane) and 12 independent detectors (room-temperature CdZnTe chips, dark count rates $\lesssim 0.001$ Hz) allowed for the collection of 12 momentum transfers simultaneously. This setup facilitates easy data collection for the longitudinal and transverse modes when the 4 (horizontal) x 3 (vertical) analyzers can be placed along a common symmetry direction [37]. The full 95 mm diameter of each analyzer crystal was used to obtain the maximum count rate, so the momentum resolution was ~ 0.1 Å^{-1} full width at half maximum (FWHM) at Si (11 11 11). The beam size on the sample was approximately 60 × 70 μm^2 (vertical × horizontal) FWHM for Si (11 11 11). For all the tasks, a slit was placed before the sample to ensure proper alignment so that the beam was incident on the sample and at the center of the spectrometer. The measured spectra were normalized using the beam intensity monitored downstream of this slit. We measured central-peak (CP) scattering and transverse-acoustic (TA) and transverse-optic (TO) modes around the (3, 0, 0) positions from −10 to 30 meV.

The temperature in all measurements was controlled between 800 and 50 K by using a high-temperature closed-cycle He-gas refrigerator. In the present experiment, the reciprocal lattice at all temperatures was set by using a primitive cubic cell ($Pm\bar{3}m$), which represents the average structure of the relaxor state of D-PIN. Because the degree of the *B*-site randomness S_2 is easy to change at high temperature, especially in the case of D-PIN, the D-PIN sample was measured only during the heating process.

III. RESULTS

A. X-ray diffuse scattering of O-PIN

Figure 3 shows the results of $H0L$ mesh scans of O-PIN at several temperatures across the transition temperature T_N. The most remarkable point is that the diffuse scattering, which is very similar to that of D-PIN [see Fig. 2(b′)], can be observed even in *ordered* PIN above T_N. Moreover, the intensity distribution of the diffuse scattering peaks at the Γ point, even far above T_N, indicating that the correlation of atomic shifts giving the diffuse scattering is ferroelectriclike. The diffuse scattering condenses mainly along the ⟨110⟩ direction as the temperature decreases toward T_N. The intensity distribution around the Γ point remains the maximum in the entire temperature region above T_N, and the intensities are suppressed suddenly below T_N (see 425 K in Fig. 3). Alternatively, the $\frac{h}{4}0\frac{l}{4}$ superlattice reflections appear below T_N.

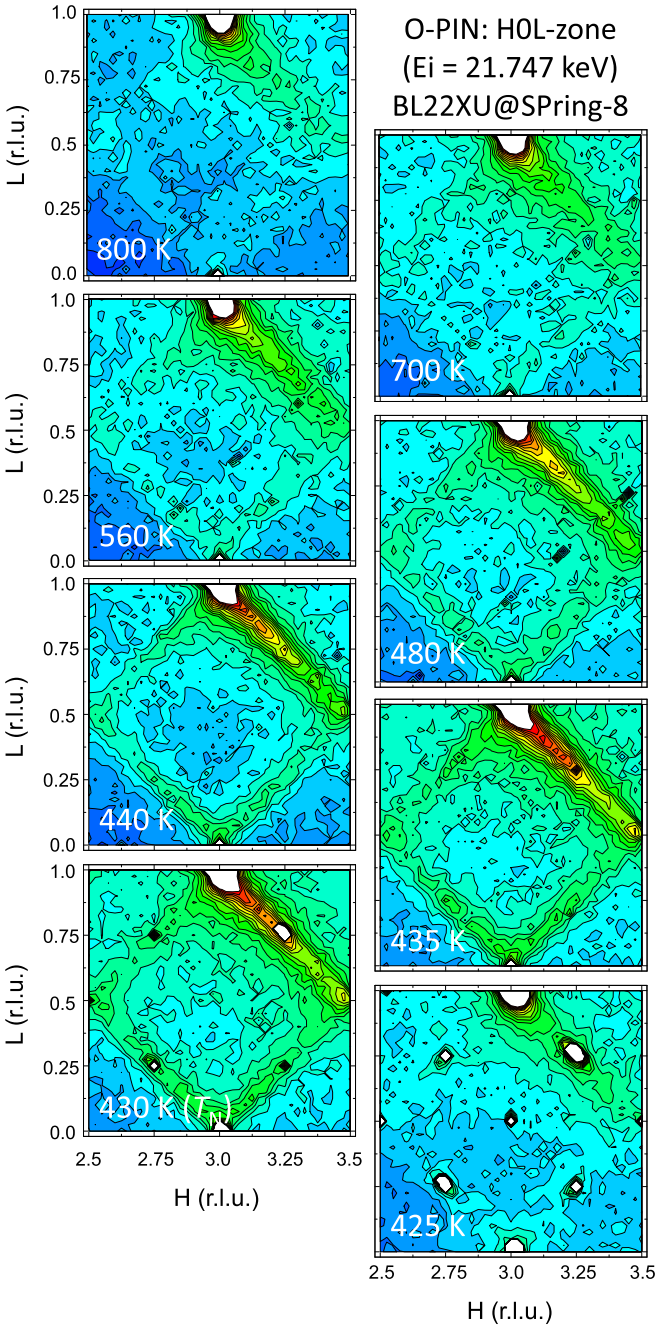

FIG. 3. $H0L$ mesh scans of O-PIN taken at 800, 700, 560, 480, 440, 435, 430, and 425 K across T_N.

Figure 4 shows the temperature dependence of the superlattice intensities and diffuse scattering intensities measured at (3.25, 0, 0.75) and (3.125, 0, 0.875), respectively. The diffuse scattering intensity gradually increases toward T_N and disappears below T_N, while the superlattice intensity appears at T_N.

Although the momentum transfers of dielectric constants (Γ point) and the diffuse scattering [$\mathbf{K} = (0.125, 0, -0.125)$] measurements are different, the temperature dependences of the dielectric constant [see Fig. 2(b)] and the diffuse scattering intensity are extremely similar.

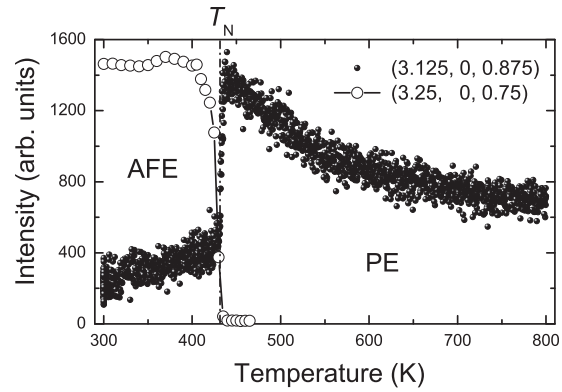

FIG. 4. Temperature dependences of superlattice intensities (open circle) and diffuse scattering intensities (solid circle) measured at (3.25, 0, 0.75) and (3.125, 0, 0.875), respectively.

This suggests that local polarization is the origin of the diffuse scattering. Furthermore, as mentioned above, the correlation of the polarization is ferroelectric.

Note that the diffuse scattering intensity I_D is proportional to the real part of the ionic susceptibility $\chi_{\text{ion}}(\mathbf{K}, \omega)$, i.e.,

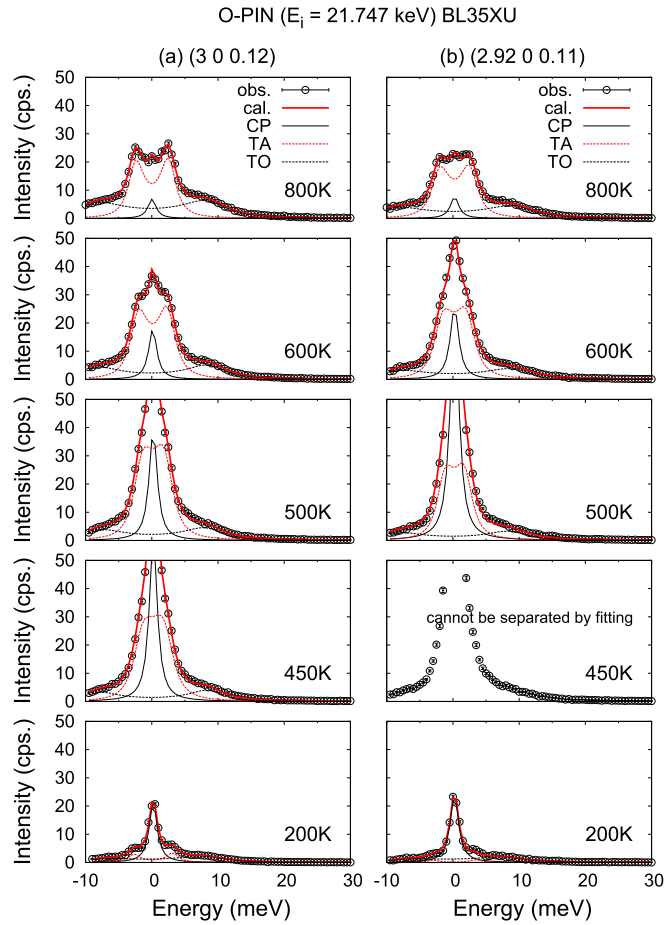

FIG. 5. Selected IXS profiles of O-PIN measurements at (a) (3, 0, 0.12) [38] and (b) (2.92, 0, 0.11) as a function of temperature. The fitting results are shown by the solid lines.

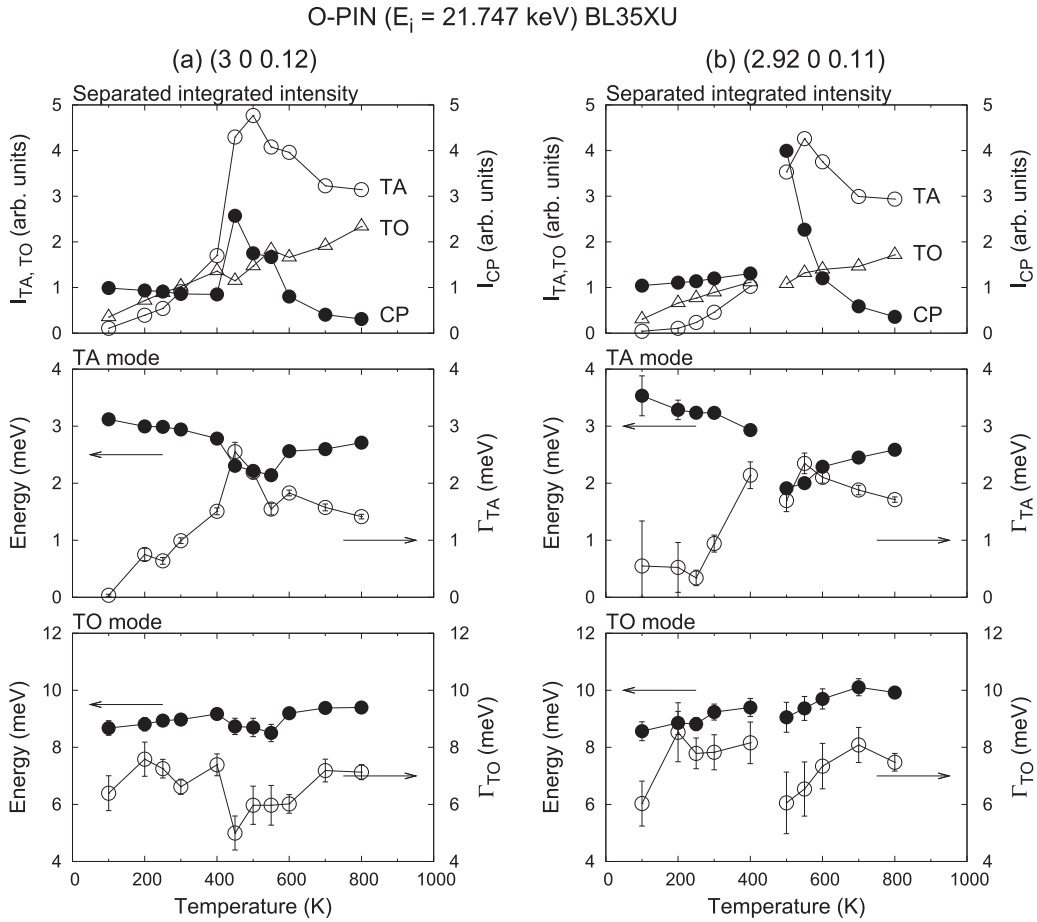

FIG. 6. Obtained fitting parameters of CP, TA, and TO modes of O-PIN at (a) (3, 0, 0.12) and (b) (2.92, 0, 0.11) as a function of temperature. The energies and widths (the middle and bottom panels) are resolution corrected.

$I_D(\mathbf{K})/T \propto \chi_{\text{ion}}(\mathbf{K}, 0)$, where all ionic-dynamic contributions are integrated.

Up to this point, it is clear that the ferroelectrically interacting local polarization exists even in the antiferroelectric O-PIN above T_N.

B. IXS measurements of O- and D-PINs

1. O-PIN

Observation of the temperature evolution of the anisotropic diffuse scattering extending along the ⟨110⟩ direction above T_N strongly suggests that the related dynamics is important for the appearance of the diffuse scattering. We therefore analyzed the diffuse scattering of O-PIN by using the IXS technique with meV resolution. Figures 5 shows the selected IXS profiles measured at (3, 0, 0.12) [Fig. 5(a)] [38] and (2.92, 0, 0.11) [Fig. 5(b)] as a function of temperature. These positions lie along the [001](Δ) and [$\bar{1}$01](Σ) lines, respectively, and correspond to the T1 and T2 branches defined in Ref. [8]. Both directions are important for investigating relaxor ferroelectrics. In this paper, we focus on the differences in the instabilities of the transverse phonons along the ⟨001⟩ and ⟨101⟩ directions. Note that the position (2.92, 0, 0.11) is slightly off the Σ line. This is due to the experimental setting for obtaining both the [001] and [$\bar{1}$01] directions in one measurement by the present IXS spectrometer with 12 pairs of analyzers and detectors. The acceptance of the analyzer was about 0.04 reciprocal lattice unit (r.l.u.); therefore, the Σ line was almost covered. The IXS data were collected during cooling. The asymmetry of the intensities on the x-ray-energy gain ($E < 0$) and loss ($E > 0$) sides, seen especially in the low-temperature region, is due to the Bose factor. The spectra are broad, indicating that strong damping exists even in the weakly chemically disordered sample O-PIN. This result shows that the strong phonon scattering mechanism exists intrinsically in this material, and this point will be discussed below.

The measured profiles were analyzed simply by using a linear combination of Lorentzian (for CP) and damped-harmonic-oscillator (for phonons) formulas [39]. The details of the formulas and the meaning of the related parameters can be found in Ref. [11]. The resolution function of the present IXS spectrometer (Lorentzian line shape) is considered as well, and the width of the CP is fixed as resolution limited, where elastic and quasielastic scattering cannot be separated. This treatment is consistent with a light-scattering measurement [31] in which the width of CP was one order of magnitude lower than the present resolution. The peak separations were almost successful, except for the data for 450 K at (2.92, 0, 0.11), where the CP was excessively strong. The coupling among the TA, TO, and CP modes was not considered.

Figure 6 shows the obtained fitting parameters of the CP, TA, and TO modes of O-PIN at (3, 0, 0.12) [Fig. 6(a)] and (2.92, 0, 0.11) [Fig. 6(b)] as a function of temperature. The top panels of Fig. 6 show the temperature dependence of the integrated intensity of the TA (I_{TA}), TO (I_{TO}), and CP (I_{CP}) components estimated from the fitting results. The results show that the major part of the diffuse scattering at high temperatures originates from the TA and TO modes, while the CP mode is dominant, especially along the [101] direction, near the critical temperature. The TO mode tends to diminish continuously as the temperature decreases. This is due to the Bose factor and not anomalous properties. The CP components increase rapidly toward T_N. By associating with the CP mode, the TA mode shows a similar increment trend toward T_N. Both modes show critical behavior, and these results indicate that the CP and TA modes are coupled. The middle panels of Fig. 6 show the temperature dependence of the energies and the damping constants Γ_{TA} of the TA modes. The energies soften slightly toward T_N and harden below T_N, in addition to showing strong damping around T_N. The damping is suppressed in the low-temperature region, indicating that the phonon scatterer stops moving. The bottom panels of Fig. 6 show the temperature dependence of the energies and the damping constants Γ_{TO} of the TO modes. No clear anomaly can be observed at T_N.

2. D-PIN

Figure 7 shows the selected IXS profiles of D-PIN measured at (3, 0, 0.12) [Fig. 7(a)] and (2.92, 0, 0.11) [Fig. 7(b)] as a function of temperature. These profiles are analyzed like those of O-PIN. Unlike the case of O-PIN, the spectrum weight around 0 meV continues to increase toward the lowest temperature. Therefore, the peaks cannot be separated by fitting in the lower-temperature region. The obtained fitting parameters of the CP, TA, and TO modes are shown in Fig. 8. The top panels of Fig. 8 show the temperature dependence of I_{TA}, I_{TO}, and I_{CP} estimated from the fitting results. Similar to O-PIN, the results show that the major part of the diffuse scattering at high temperatures can be ascribed to the TA and TO modes, and that at low temperatures can be ascribed to the CP mode. There is no clear difference between O- and D-PIN in the high-temperature regions. The TO mode also tends to decrease continuously toward low temperatures. The CP components increase rapidly toward low temperatures. By associating with the CP mode, the TA mode shows anomalous temperature change, and it does not decrease continuously, unlike the TO mode. The trend changes clearly at approximately 500 K, where the temperature corresponds to $T^* \sim 475$ K of D-PIN [31]. These results indicate that the coupling between the CP and the TA modes is maintained even in D-PIN. The middle panels of Fig. 8 show the temperature dependence of the energies and the damping constants Γ_{TA} of the TA modes. Compared to the results for O-PIN, the energies do not show clear softening, but strong damping can be observed in the same region as that in the case of O-PIN. The bottom panels of Fig. 8 show the temperature dependence of the energies and the damping constants Γ_{TO} of the TO modes. No clear anomaly can be observed, in common with O-PIN.

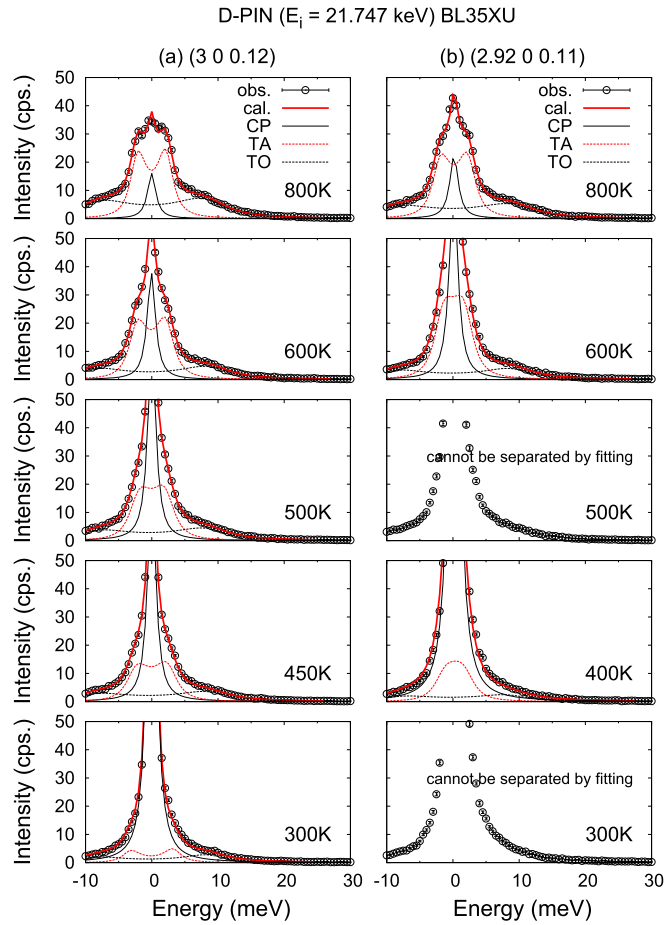

FIG. 7. Selected IXS profiles of D-PIN measurements at (a) (3, 0, 0.12) and (b) (2.92, 0, 0.11) as a function of temperature. Fitting results are shown by the solid lines. Owing to the contribution of strong elastic scattering, the IXS profiles cannot be separated by fitting, especially in the lower-temperature region.

IV. DISCUSSION

A. Polarization fluctuation: Origin of the central peak

As discussed in Sec. III A, the diffuse scattering measurement of O-PIN shows that the ferroelectrically interacting local polarization exists even in the antiferroelectric O-PIN above T_N. An IXS analysis of the diffuse scattering showed that the TA and TO modes are dominant in the case of diffuse scattering at high temperatures, while the CP and TA modes, which are coupled, contribute majorly to the diffuse scattering near T_N and show critical behavior toward T_N. The TO mode shows no anomaly toward T_N. Because the TA mode is a *strain* mode, the CP mode is naively considered to be related to the local polarization near T_N. Furthermore, the phonon spectra are broad, indicating that strong damping mechanisms exist even in the weakly chemically disordered sample O-PIN.

To understand the dynamic nature of O-PIN, it is useful to compare it with $PbZrO_3$ (PZO). The structure [40–42], dynamics [43], and diffuse scattering [43] are similar to those of O-PIN.

It is widely known that Pb atoms are randomly off centered around the *A* site in lead-based relaxor materials, including PIN systems [41,44]. Interestingly, such *A*-site off-centeredness is

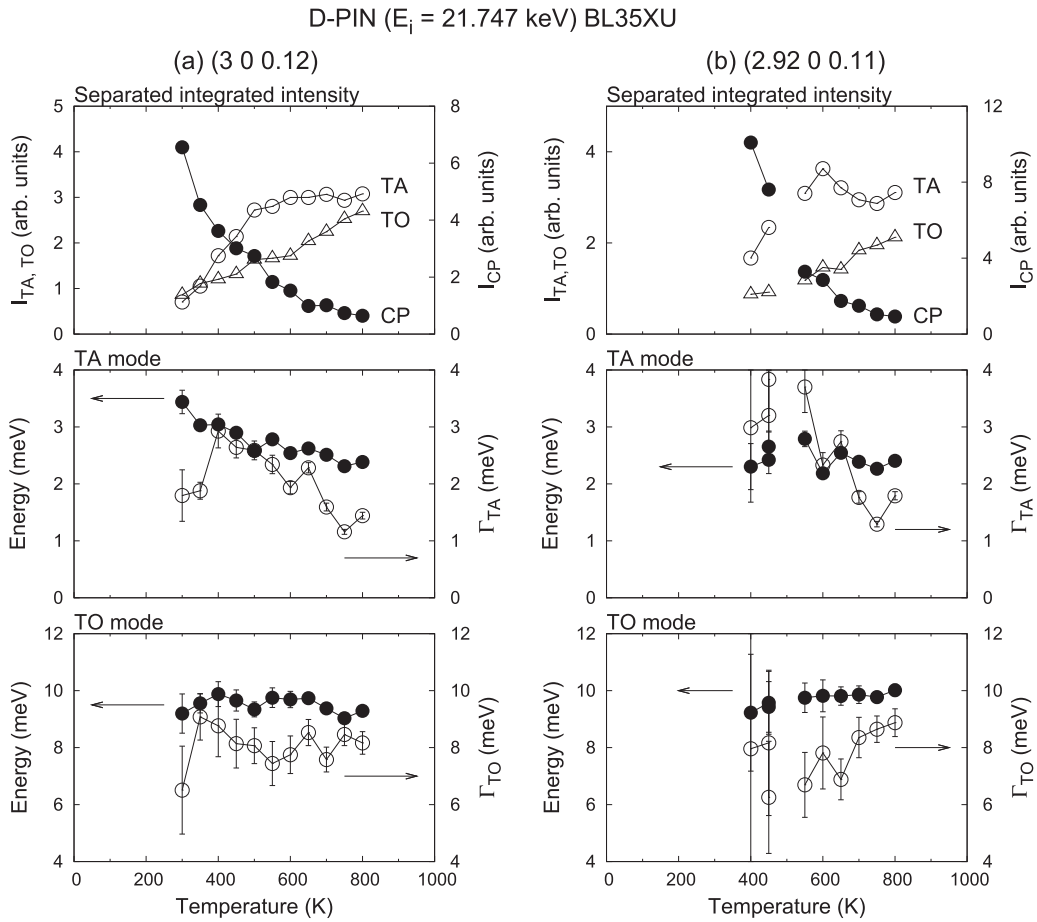

FIG. 8. Obtained fitting parameters of CP, TA, and TO modes of D-PIN at (a) (3, 0, 0.12) and (b) (2.92, 0, 0.11) as a function of temperature. The energies and widths (the middle and bottom panels) are resolution corrected.

inherent in lead-based *antiferroelectric* materials with a simple perovskite structure, such as PZO and $PbHfO_3$, while the *A*-site off-centeredness is not found in the prototypical FE material $PbTiO_3$ [45,46]. The importance of the *A*-site off-centeredness of the Pb atoms in relaxors has been discussed in many works [20,47–49].

The energy dispersion of the lowest-energy TO mode, the polarization mode, in PINs has already been observed to decrease toward the Γ point in spite of *B*-site randomness [11], indicating that a dynamic ferroelectric correlation exists in the basis of the PIN system.

As shown schematically in Fig. 9, the strongly off-centered Pb-flipping motion can be affected by the TO mode and results in the ferroelectric correlation. From another perspective, the TO mode is strongly scattered by the randomly flipping Pb ions, which is observed as strong damping.

Yamada *et al.* [50] developed an argument to explain the change in the phonon spectrum under the pseudospin-phonon coupling. In this case, the Pb-flipping motion corresponds to the pseudospin. When the relaxation rate of the Pb flipping is comparable to the TO phonon frequency, both the CP and TO modes are broad, and the CP mode shows critical slowing-down behavior, while the TO mode shows only a weak change. Burkovsky *et al.* [43] also pointed out the coupling between soft TO and a relaxing degree of freedom ("rattling" of the Pb ion is suggested in their paper) can generate CP in PZO.

Such a mechanism should be considered when the CP mode exhibits the nature of local polarization. Matsuura *et al.* [51] successfully applied Yamada *et al.*'s model [50] to analyze the precisely measured neutron inelastic spectrum of PMN-30%PT. As this work demonstrates, more detailed experiments over a wide energy range from μeV to meV are needed in the present PIN series to clarify the CP-TO relationship. Furthermore, the fractal (or power law) nature [31,52,53] should additionally be considered in the temperature region

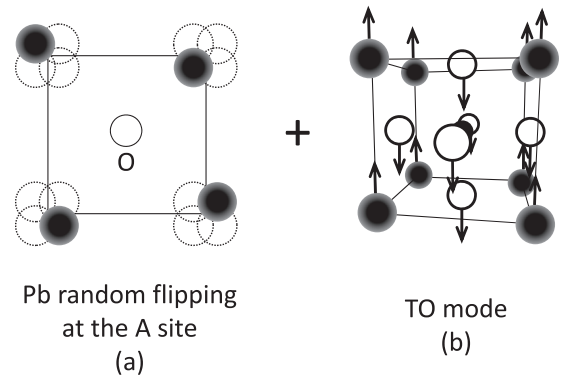

FIG. 9. Schematic drawing of (a) Pb-flipping motion and (b) the TO phonon (last) mode. Their mutual interaction is strong.

where the CP mode is dominant, for example, below T^* in the case of D-PIN.

B. Role of the *B* site: Control of AFE/FE instability

The O-PIN system transforms into the AFE phase, even though the system has a strong ferroelectric correlation. The TA mode shows slight softening and hardening across T_N, and finally, $(\frac{h}{4}\frac{k}{4}0)$-type superlattice reflections appear. From the measurement along the Δ and Σ lines, phonon instability can be seen in the wide Brillouin zone around the zone center (Γ point). Generally, mode condensation at a momentum transfer $\mathbf{k}_0$ (equal to mode instability at $\mathbf{k}_0$) is a result of complex interatomic interactions, namely, the intricate balance between short-range repulsive (e.g., covalent bonding) and long-range (Coulomb) interactions [54], inside materials.

Similar to O-PIN, the diffuse scattering intensity is distributed widely on the Σ line in PZO. It has been suggested that the phonon branch on the Σ line is unstable [43,55]. TA-(soft) TO flexoelectric mode coupling [42,43] has been proposed to drive such a finite-$\mathbf{k}_0$ (AFE) instability. In this circumstance, antiphase Pb shift and octahedron rotation/tilt take place. Generally, such mode instability could also drive an AFE phase with a longer period in materials such as $Pb(Yb_{1/2}Nb_{1/2})O_3$ (commensurate structure) [28] and $Pb(Co_{1/2}W_{1/2})O_3$ (incommensurate structure) [56].

As shown in Fig. 1, the ionic radii at the perovskite *B* site contribute to the AFE/FE nature of the Pb-based perovskites. The average ionic radius of the *B* site of O-PIN (0.72 Å) is the same as that of PZO. The environments of both O-PIN and PZO are very similar on average. In the case of Pb-based perovskites showing the AFE phase transition, spatial margins around the *A* site are large, but they are small around the *B* site. The *limiting* environment around the perovskite *B* site drives the octahedral rotation/tilt (corresponding to the *M*, *R* mode softening) against the *B*-O covalent bond. In contrast, the *free* environment around the perovskite *A* site drives the Pb flipping around the *A* site and strengthens the covalent bond with the neighboring oxygen [45,57].

However, in the case of O-PIN, unlike PZO, there will be a $2a \times 2b \times 2c$ staggered field owing to the difference in charge/ionic radius between In^{2+} and Nb^{5+}. The AFE phase-transition temperatures of PZO and O-PIN are 505 and 425–450 K, respectively. There is a possibility that the ionic radius difference hinders the tilt/rotation of the octahedron in O-PIN; in other words, covalent character is enhanced due to the existence of two kinds of ions, especially the Nb^{5+} ion with its small ionic radius of 0.64 Å.

C. Effect of *B*-site randomness: Enhancement of polarization fluctuation

Finally, the effect of *B*-site randomness is discussed. As mentioned above, the dynamics is independent of the *B*-site randomness in the high-temperature region. This is consistent with the finding of a previous report that "no influence of the size of compositionally ordered regions (CORs) on the polar nanoregions (PNRs) relaxation in the ergodic relaxor phase is found" [58]. In the present paper, at least two effects of the *B*-site randomness can be proposed. One is suppression of the finite-$\mathbf{k}_0$ instability (AFE), and the other is enhancement of the polarization fluctuation.

For the first effect, as mentioned in Ref. [11], the randomness weakly affects the FE correlation because it is a long-wavelength fluctuation. By contrast, the AFE instability, a short-wavelength (finite-$\mathbf{k}_0$) TA instability, can easily be affected by the randomness. In other words, the short-range repulsive interaction associated with the covalent bond is locally enhanced by the randomness, which results in suppression of the antiferroelectricity [54]. Therefore, the polar regions tend to appear as the randomness increases. Such a heterogeneous bonding nature was proposed in the relaxor ferroelectrics PMN-*x*PT to be ionic around the Mg ion but covalent around the Ti and Nb ions [59].

In the case of the second effect, as clearly seen in the dielectric measurement (see Figs. 2(b) and 2(c) [23] and a previous report [25]), the dielectric constants of the D-PIN are larger than those of O-PIN even if we compare them at the same temperature and measurement frequencies above T_N. This trend is especially apparent in the case of $B' = Sc$ [20]. At the time of their formation, the polar regions contain randomly oriented local electric fields. These fields enhance the instability of the polarization fluctuation of the polar regions and enhance the dielectric susceptibility. This scenario was demonstrated by Tomita *et al.* via Monte Carlo simulations [60,61]. As previously discussed in Sec. IV A, the origin of the CP mode is local polarization. Therefore, the present result that the CP components of D-PIN are larger than those of O-PIN is in agreement with the results of the dielectric measurements [23,25].

V. SUMMARY

We have investigated the effect of *B*-site randomness on the antiferroelectric/relaxor nature of the ground state by studying diffuse and inelastic x-ray scattering from O- and D-PIN single crystals.

The diffuse scattering measurement of O-PIN, which is antiferroelectric at low temperatures, shows that the ferroelectrically interactive local polarization exists in the cubic phase, above the transition temperature T_N. The IXS analysis of the diffuse scattering showed that the TA and TO modes were dominant at high temperatures (~800 K), while the CP and TA modes, which are mutually coupled, contributed majorly to the diffuse scattering near T_N and showed critical behavior at temperature close to T_N. The TO mode showed no anomaly at temperature close to T_N. Furthermore, the phonon spectra were broad, indicating that strong damping exists even in the weakly chemically disordered sample, O-PIN. No clear difference between O- and D-PIN was observed at temperatures above ~500 K. The coupling between CP and TA could be observed. The major difference was the property of the CP mode, which showed no drop and increased rapidly with decreasing temperatures. To investigate the properties of the CP mode precisely in the low-temperature region, μeV energy resolution will be required.

The CP mode was discussed as being related directly to the local polarization and to originate in the combination of Pb flipping and the TO mode. The *B* site is thought to control the AFE/FE instability of lead-based perovskite materials. Finally, the effect of the *B*-site randomness was discussed in terms of

suppressing the AFE instability and enhancing the polarization fluctuation.

ACKNOWLEDGMENTS

We would like to thank Dr. Y. Tomita (Shibaura Institute of Technology), Dr. J. Harries (QST), Dr. Y. Uesu (professor emeritus at Waseda University), Dr. H. Taniguchi (Nagoya University), Dr. M. Iwata (Nagoya Institute of Technology), Dr. S. Mori (Osaka Prefecture University), Dr. Y. Fujii (professor emeritus at the University of Tokyo), and the late Dr. K. Hirota and the late Dr. G. Shirane for discussions and comments. This work was partly supported by a Grant-in-Aid for Scientific Research on Priority Areas "Novel States of Matter Induced by Frustration" (JP19052002). The XDS and IXS experiments were performed at SPring-8 with the approval of the Japan Synchrotron Radiation Research Institute (JASRI) (Proposals No. 2013B3713, No. 2011A3713, No. 2010A1459, No. 2009B3713, and No. 2009A1203).

[1] G. A. Smolenskii, A. I. Agronovskaya, and S. N. Popov, Fizika Tverd. Tela **2**, 2906 (1960) [Sov. Phys. Solid State **2**, 2584 (1961)].
[2] J. Hlinka, J. Adv. Dielectr. **02**, 1241006 (2012).
[3] H. Takenaka, I. Grinberg, S. Liu, and A. M. Rappe, Nature (London) **546**, 391 (2017).
[4] P. M. Gehring, K. Ohwada, and G. Shirane, Phys. Rev. B **70**, 014110 (2004).
[5] G. Xu, P. M. Gehring, and G. Shirane, Phys. Rev. B **72**, 214106 (2005).
[6] G. Xu, J. Wen, C. Stock, and P. M. Gehring, Nat. Mater. **7**, 562 (2008).
[7] Z. Xu, J. Wen, G. Xu, C. Stock, J. S. Gardner, and P. M. Gehring, Phys. Rev. B **82**, 134124 (2010).
[8] J. A. Schneeloch, Z. Xu, B. Winn, C. Stock, P. M. Gehring, R. J. Birgeneau, and G. Xu, Phys. Rev. B **92**, 214302 (2015).
[9] D. Shimizu, S. Tsukada, M. Matsuura, J. Sakamoto, S. Kojima, K. Namikawa, J. Mizuki, and K. Ohwada, Phys. Rev. B **92**, 174121 (2015).
[10] K. Ohwada, S. Tsukada, M. Matsuura, T. Satoshi, A. Q. R. Baron, J. Mizuki, and K. Namikawa, Ferroelctrics (to be published).
[11] K. Ohwada, K. Hirota, H. Terauchi, T. Fukuda, S. Tsutsui, A. Q. R. Baron, J. Mizuki, H. Ohwa, and N. Yasuda, Phys. Rev. B **77**, 094136 (2008).
[12] D. Phelan, C. Stock, J. A. Rodriguez-Rivera, S. Chi, J. Leão, X. Long, Y. Xie, A. A. Bokov, Z.-G. Ye, P. Ganesh *et al.*, Proc. Natl. Acad. Sci. USA **111**, 1754 (2014).
[13] V. Westphal, W. Kleemann, and M. D. Glinchuk, Phys. Rev. Lett. **68**, 847 (1992).
[14] R. Pirc and R. Blinc, Phys. Rev. B **60**, 13470 (1999).
[15] Y. Hotta, G. W. J. Hassink, T. Kawai, and H. Tabata, Jpn. J. Appl. Phys. **42**, 5908 (2003).
[16] R. Shannon, Acta Crystallogr. A **32**, 751 (1976); http://abulafia.mt.ic.ac.uk/shannon/.
[17] Y. Fujii, N. Wakiya, J.-H. Lim, O. Sakurai, K. Shinozaki, and N. Mizutani, J. Ceram. Soc. Jpn. **104**, 691 (1996).
[18] Y. Park, Solid State Commun. **113**, 379 (2000).
[19] H. Sim, D. C. Peets, S. Lee, S. Lee, T. Kamiyama, K. Ikeda, T. Otomo, S.-W. Cheong, and J.-G. Park, Phys. Rev. B **90**, 214438 (2014).
[20] C. Malibert, B. Dkhil, J. M. Kiat, D. Durand, J. F. Berar, and A. S. de Bire, J. Phys.: Condens. Matter **9**, 7485 (1997).
[21] O. Bidault, C. Perrin, C. Caranoni, and N. Menguy, J. Appl. Phys. **90**, 4115 (2001).
[22] C. Perrin, N. Menguy, O. Bidault, C. Y. Zahra, A.-M. Zahra, C. Caranoni, B. Hilczer, and A. Stepanov, J. Phys.: Condens. Matter **13**, 10231 (2001).
[23] H. Ohwa, M. Iwata, H. Orihara, N. Yasuda, and Y. Ishibashi, J. Phys. Soc. Jpn. **69**, 1533 (2000).
[24] A. A. Bokov, V. Y. Shonov, I. P. Rayevsky, E. S. Gagarina, and M. F. Kupriyanov, J. Phys.: Condens. Matter **5**, 5491 (1993).
[25] M. Iwata, S. Katagiri, H. Orihara, M. Maeda, I. Suzuki, H. Ohwa, N. Yasuda, and Y. Ishibashi, Ferroelectrics **301**, 179 (2004).
[26] X. Yang, Y. Liu, C. He, H. Tailor, and X. Long, J. Eur. Ceram. Soc. **35**, 4173 (2015).
[27] N. Yasuda and H. Inagaki, Jpn. J. Appl. Phys. **30**, L2050 (1991).
[28] J.-R. Kwon and W.-K. Choo, J. Phys.: Condens. Matter **3**, 2147 (1991).
[29] Y. Park, J. Phys. Chem. Solids **59**, 1423 (1998).
[30] K. Nomura, T. Shingai, N. Yasuda, H. Ohwa, and H. Terauchi, J. Phys. Soc. Jpn. **68**, 866 (1999).
[31] S. Tsukada, K. Ohwada, H. Ohwa, S. Mori, S. Kojima, N. Yasuda, H. Terauchi, and Y. Akishige, Sci. Rep. **7**, 17508 (2017).
[32] A. A. Bokov, I. P. Raevskii, and V. G. Smotrakov, Fiz. Tverd. Tela **26**, 2824 (1984) [Sov. Phys. Solid State **26**, 1708 (1984)].
[33] N. Yasuda, H. Ohwa, J. Oohashi, K. Nomura, H. Terauchi, M. Iwata, and Y. Ishibashi, J. Phys. Soc. Jpn. **67**, 3952 (1998).
[34] K. Nomura, T. Shingai, S. Ishino, H. Terauchi, N. Yasuda, and H. Ohwa, J. Phys. Soc. Jpn. **68**, 39 (1999).
[35] K. Nomura, N. Yasuda, H. Ohwa, and H. Terauchi, J. Phys. Soc. Jpn. **66**, 1856 (1997).
[36] T. Shobu, K. Tozawa, H. Shiwaku, H. Konishi, T. Inami, T. Harami, and J. Mizuki, in *Synchrotron Radiation Instrumentation: Ninth International Conference on Synchrotron Radiation Instrumentation*, edited by J.-Y. Choi and S. Rah, AIP Conf. Proc. No. 879 (AIP, New York, 2007), p. 902.
[37] A. Q. R. Baron, Y. Tanaka, S. Goto, K. Takeshita, T. Matsushita, and T. Ishikawa, J. Phys. Chem. Solids **61**, 461 (2000).
[38] K. Ohwada, T. Fukuda, J. Mizuki, K. Hirota, H. Terauchi, S. Tsutsui, A. Q. R. Baron, H. Ohwa, and N. Yasuda, J. Korean Phys. Soc. **59**, 2509 (2011).
[39] B. Fåk and B. Dorner, Phys. B (Amsterdam, Neth.) **234**, 1107 (1997).
[40] P. Groves, Phase Transitions **6**, 115 (1986).
[41] Y. Yoneda, K. Suzuya, J. Mizuki, and S. Kohara, J. Appl. Phys. **100**, 093521 (2006).
[42] A. K. Tagantsev, K. Vaideeswaran, S. B. Vakhrushev, A. V. Filimonov, R. G. Burkovsky, A. Shaganov, D. Andronikova, A. I. Rudskoy, A. Q. R. Baron, H. Uchiyama *et al.*, Nat. Commnun. **4**, 2229 (2013).
[43] R. G. Burkovsky, A. K. Tagantsev, K. Vaideeswaran, N. Setter, S. B. Vakhrushev, A. V. Filimonov, A. Shaganov, D. Andronikova, A. I. Rudskoy, A. Q. R. Baron *et al.*, Phys. Rev. B **90**, 144301 (2014).

[44] S. G. Zhukov, A. V. Yatsenko, and S. B. Vakhrushev, J. Struct. Chem. **38**, 486 (1997).
[45] Y. Kuroiwa, H. Fujiwara, A. Sawada, S. Aoyagi, E. Nishibori, M. Sakata, M. Takata, H. Kawaji, and T. Atake, Jpn. J. Appl. Phys. **43**, 6799 (2004).
[46] Y. Kuroiwa, Y. Terado, and C. Moriyoshi, Ferroelectrics **354**, 158 (2007).
[47] Y. Uesu, H. Tazawa, K. Fujishiro, and Y. Yamada, J. Korean Phys. Soc. **29**, S703 (1996).
[48] Y. Terado, S. J. Kim, C. Moriyoshi, Y. Kuroiwa, M. Iwata, and M. Takata, Jpn. J. Appl. Phys. **45**, 7552 (2006).
[49] M. Paściak, T. R. Welberry, J. Kulda, M. Kempa, and J. Hlinka, Phys. Rev. B **85**, 224109 (2012).
[50] Y. Yamada, H. Takatera, and D. L. Huber, J. Phys. Soc. Jpn. **36**, 641 (1974).
[51] M. Matsuura, H. Hiraka, K. Yamada, and K. Hirota, J. Phys. Soc. Jpn. **80**, 104601 (2011).
[52] A. Koreeda, H. Taniguchi, S. Saikan, and M. Itoh, Phys. Rev. Lett. **109**, 197601 (2012).
[53] S. Vakhrushev, A. Nabereznov, S. Sinha, Y. Feng, and T. Egami, J. Phys. Chem. Solids **57**, 1517 (1996).
[54] G. A. Samara, T. Sakudo, and K. Yoshimitsu, Phys. Rev. Lett. **35**, 1767 (1975).
[55] J. Hlinka, T. Ostapchuk, E. Buixaderas, C. Kadlec, P. Kuzel, I. Gregora, J. Kroupa, M. Savinov, A. Klic, J. Drahokoupil *et al.*, Phys. Rev. Lett. **112**, 197601 (2014).
[56] S. Watanabe and Y. Koyama, Phys. Rev. B **65**, 064108 (2002).
[57] S. Aoyagi, Y. Kuroiwa, A. Sawada, H. Tanaka, J. Harada, E. Nishibori, M. Takata, and M. Sakata, J. Phys. Soc. Jpn. **71**, 2353 (2002).
[58] A. A. Bokov, B. J. Rodriguez, X. Zhao, J.-H. Ko, S. Jesse, X. Long, W. Qu, T.-H. Kim, J. D. Budai, A. N. Morozovska *et al.*, Z. Kristallogr. **226**, 99 (2011).
[59] L. Bellaiche and D. Vanderbilt, Phys. Rev. Lett. **83**, 1347 (1999).
[60] Y. Tomita, T. Kato, and K. Hirota, J. Phys. Soc. Jpn. **79**, 023001 (2010).
[61] K. Ohwada and Y. Tomita, J. Phys. Soc. Jpn. **79**, 011012 (2010).